Photon antibunching in double quantum ring structures

M. Abbarchi,[1,*] C. A. Mastrandrea,[1] A. Vinattieri,[1] S. Sanguinetti,[2] T. Mano,[3] T. Kuroda,[3] N. Koguchi,[2] K. Sakoda,[3] and M. Gurioli[1]

[1]*Dipartimento di Fisica, CNISM, Università di Firenze and European Laboratory for Non-Linear Spectroscopy, Via Sansone 1, 50019 Sesto Fiorentino (Firenze), Italy*

[2]*Dipartimento di Scienza dei Materiali and LNESS, Università di Milano Bicocca, Via Cozzi 53, 120125 Milano, Italy*

[3]*National Institute for Materials Science, 1-1 Namiki, Tsukuba 305-0044, Japan*

(Received 1 July 2008; revised manuscript received 11 November 2008; published 11 February 2009)

We address the question whether a quantum ring nanostructure can be considered as a single-photon emitter by means of intensity time-correlation measurement based on a Hanbury-Brown and Twiss interferometer. The second-order correlation function $g^{(2)}$ well characterizes the quantum nature of the emitter by the photon antibunching dip at zero delay. In concentric quantum rings we find evidence that the inner ring satisfies the requirement of single-photon source, while in the outer ring this requirement is relaxed.

DOI: 10.1103/PhysRevB.79.085308 PACS number(s): 78.67.−n, 73.21.−b, 78.55.Cr

I. INTRODUCTION

Quantum mechanical phenomena in ring geometries have fascinated for a long time the physics community. Electrons confined in nanometric rings manifest a topological quantum interference phenomenon known as Aharonov-Bohm effect.[1] The ground-state energy of a charged particle oscillates with the magnetic field, with an oscillation period given in unity of the magnetic quantum flux h/e. Recently, the ability to fill a nanometric ring with few electrons has offered the possibility to experimentally detect such effect by magnetization experiments of the oscillatory persistent currents carried by single electron states.[2] Exciton (X) Aharonov-Bohm effect has been predicted as well due to the exciton nonzero electric dipole moment.[3] In particular type-II quantum rings have been expected to be particularly amenable to exhibit the effect due to the spatial separation of electrons and holes, as recently observed in ZnSe quantum rings.[4] On the other hand the recent success in self-assembled nucleation of double concentric quantum rings (CQRs) (Ref. 5) has provided suitable nanostructures for exploring the magneto-optical excitations on the basis of the Rashba spin-orbit interaction.[6] Quantum rings have a peculiar and useful magnetic field level dispersion; unlike quantum dots (QDs) the ground-state total angular momentum changes from zero to nonzero by increasing the magnetic field.[7,8] This also results in a different energy dispersion of the excitons for different ring radius. Since charge tunneling between states of different angular momentum is strongly suppressed by selection rules, double concentric quantum rings eventually offer the control of effective coupling of direct-indirect excitons,[9] which is of the utmost relevance in the research of semiconductor-based quantum computational devices.

All these fascinating phenomena consider the quantum ring as an ideal quantum system. However, to realize semiconductor quantum devices disorder cannot be neglected. Disorder-related effects are largely discussed in quantum well and quantum wire literature, leading to the concept of exciton localization.[10] In quantum dots disorder is extremely relevant in devices operating over a large ensemble of QDs; the size and shape are not fully controllable in the self-assembled growth and large size dispersion is found.[11] However for each single quantum dot the carrier confinement occurs over a spatial region much smaller than the exciton Bohr radius. Therefore the disorder does not play a major role and the single QD optical transitions are well described in terms of a two-level system. This is clearly demonstrated by antibunching experiments on the excitonic recombination where $g^{(2)}(\tau=0)=0$ has been measured.[12–14] In the case of quantum rings the length of the circumference is usually larger than the exciton Bohr radius. This means that quantum rings, due to their rather peculiar annular shape, possess an electronic structure which is a crossover between the dot and the wire case. As recently suggested, a large quantum ring can be considered as a warped analogous to quantum wires and disorder can play a relevant role even for a single nanostructure.[15]

In this paper we precisely address the point whether a quantum ring nanostructure can be considered as an ideal quantum system by probing its reliability as a single-photon source. The experimental method is the intensity time correlation based on a Hanbury-Brown and Twiss (HBT) interferometer. In fact the second-order correlation function $g^{(2)}$ well characterizes the quantum nature of the emitter by the presence or not of photon antibunching.[14] In CQRs we find evidence that the inner ring (IR) satisfies the requirement of quantum emitter of single photons, while in the outer ring (OR) this requirement is not fulfilled.

II. SAMPLE GROWTH AND EXPERIMENTAL DETAILS

GaAs CQRs were grown on $Al_{0.3}Ga_{0.7}As$ using modified droplet epitaxy (MDE).[5] In MDE, Ga atoms are supplied solely in the initial stage of growth, producing nanometer-sized droplets. After formation of the Ga droplets, As atoms are supplied, leading to droplets crystallization into GaAs nanocrystals. In contrast to the other methods to fabricate QDs, such as Stranski-Krastanov growth, this technique can produce strain-free quantum dots based on lattice-matched heterosystems. MDE allows for a high controllability of the crystalline shape, via the As flux, from conelike to CQR structures characterized by an inner and an outer ring.[5] The

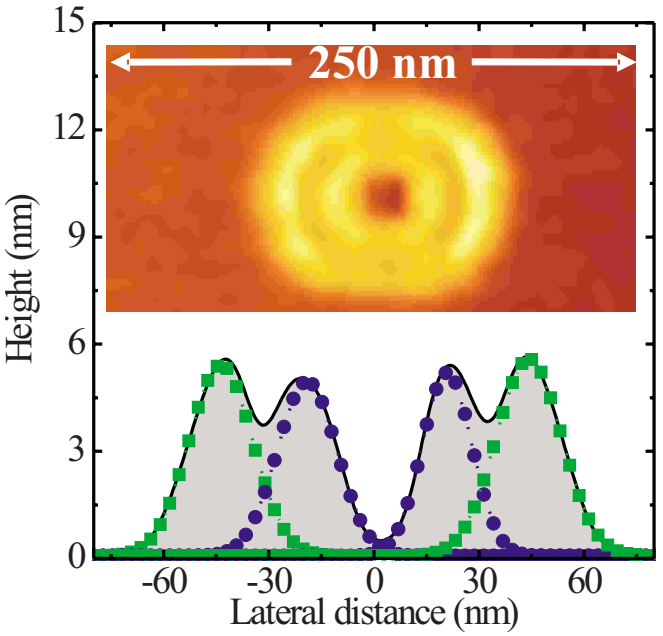

FIG. 1. (Color online) Cross section of the AFM image of inset. Inset: typical AFM image of a GaAs CQR. The CQRs show good circular symmetry, whereas a small elongation is found along the $[1\bar{1}0]$ direction. The inner ring dimensions are 40 nm diameter with 5.2 nm height, and the outer ring dimensions are 90 nm diameter with 5.6 nm height. The squares and the circles represent the Gaussian fit to the section profiles of the outer and inner rings, respectively. The full width at half maximum (FWHM) of OR and IR are 21 and 18 nm, respectively.

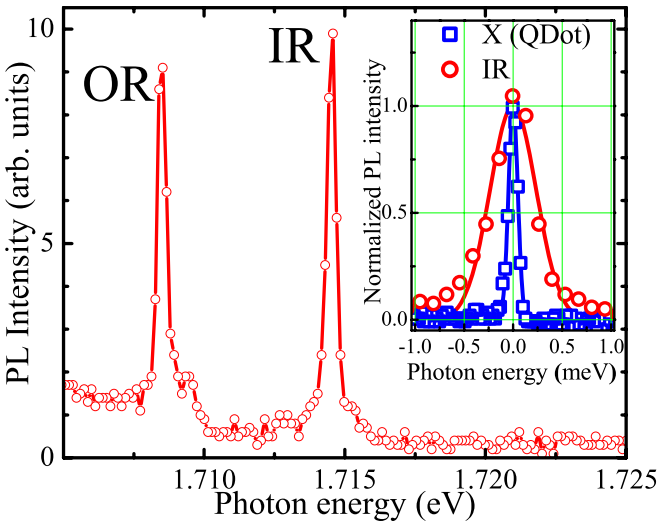

FIG. 2. (Color online) Typical PL spectrum of a CQR. The two lines labeled as IR and OR are related to the excitonic emission from inner and outer rings, respectively. Inset: comparison between the neutral exciton recombination (X, squares) in a GaAs QD and the inner ring exciton (IR, circles) recombination in a CQR. The two measured linewidths (FWHM) are 110 and 550 μeV for the QD and CQR, respectively (the spectra are shifted in energy and normalized for an easier comparison).

CQR sample studied here was obtained by depositing Ga droplets [1.75 monolayer (ML) of Ga at 0.05 ML/s on the surface of an $Al_{0.3}Ga_{0.7}As$ substrate at 300 °C] followed by the irradiation with 2×10^{-6} Torr beam equivalent pressure of As at 200 °C. The CQRs have been characterized before capping by atomic force microscopy (AFM), as shown in the inset of Fig. 1. The cross section of the AFM image, together with Gaussian fits, is also reported in Fig. 1. The CQRs show a good circular symmetry, whereas small elongation is found along the $[1\bar{1}0]$ direction (5% for the inner ring and 8% for the outer ring). The inner ring dimensions are 40 nm diameter and 5.2 nm height, and the outer ring has 90 nm diameter with 5.6 nm height. The CQR density is 1.3×10^{8} cm^{-2}, thus allowing the capture of the emission from a single CQR structure using a micro-objective setup. After ring formation, the sample was capped by an $Al_{0.3}Ga_{0.7}As$ barrier of 100 nm thickness. A thick (Al,Ga)As layer completes the structure. The samples underwent a rapid thermal annealing (RTA) at 750 °C for 4 min to improve their optical quality. Note that the final RTA processing does not modify the nanocrystalline ring shape, according to the negligible interdiffusion of Ga and As at the GaAs/(Al,Ga)As heterointerface at the relevant temperature.

We performed photoluminescence (PL) measurements for several different single CQRs under nonresonant excitation in the AlGaAs barrier. For excitation, second-harmonic output of a mode-locked Ti-sapphire laser was employed. The laser provided femtosecond pulses at 400 nm of wavelength and 82.0 MHz repetition rate. The sample was placed in a cold-finger helium flow cryostat, and microphotoluminescence (μ-PL) measurements were performed in the far field using a microscope objective with 0.7 numerical aperture to detect individual nanostructures. For the collection, a confocal configuration of two infinity corrected microscope objectives was used. The PL signal was coupled to a single-mode optical fiber of 5 μm core diameter and then split by a 50/50 beam splitter. Then, each beam was fed into a grating monochromator [250 μeV resolution expressed as FWHM in the following] equipped with a silicon avalanche photodiode (APD). Electric pulses from the two APDs were sent to a time-correlated single-photon counting setup, each pulse acting as a start or stop event for the coincidence measurement of an HBT interferometer, providing an experimental resolution of 660 ps (FWHM). PL spectra were measured using a cooled charge-coupled device. All experiments were performed at 15 K.

III. EXPERIMENTAL RESULTS

Figure 2 reports the typical photoluminescence spectrum of an individual CQR. In the low excitation regime we always observe a doublet, whose components are separated by several meV. The doublet structure of the emission has been attributed[16] to the emissions of IR and OR of the CQR based on the effective-mass model where the confining potential was modeled on the AFM analysis. The physical reason of the splitting between IR and OR optical transitions only partially relies in the different length of the ring. A major contribution arises from the different widths of the two rings. From the AFM investigation (see Fig. 1), it emerges that the

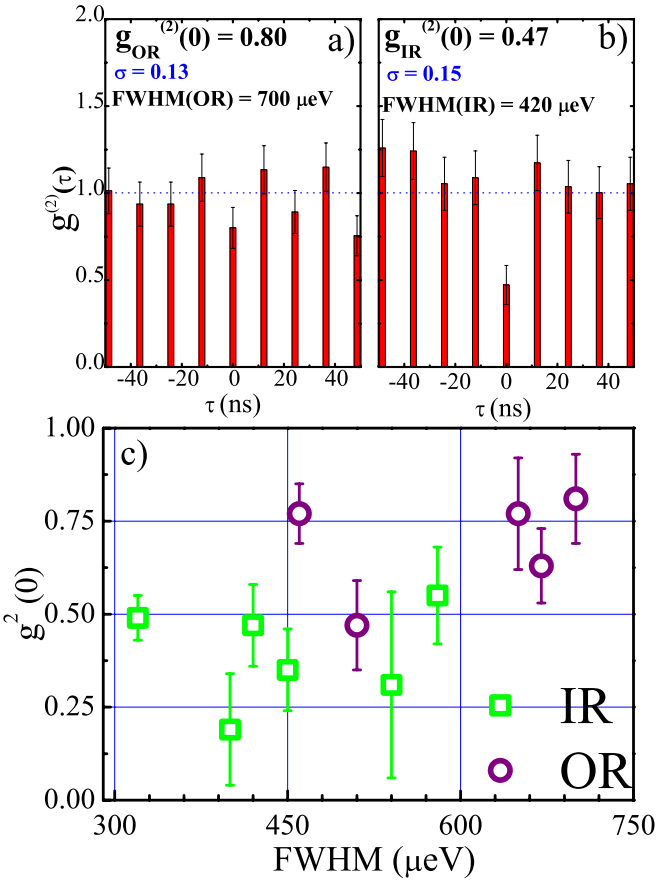

FIG. 3. (Color online) (a) and (b) are pulsed excitation measurement of $g^{(2)}(\tau)$ for OR and IR, respectively. The error bar associated to each peak is the coincidence count square root normalized to the average value of the peaks intensity. σ is the standard deviation of the average value of the peak intensity (except for the zero-delay one). (c) Summary of all the measured $g^{(2)}(0)$ for IR (squares) and OR (circles); the error bars are the measured standard deviation σ.

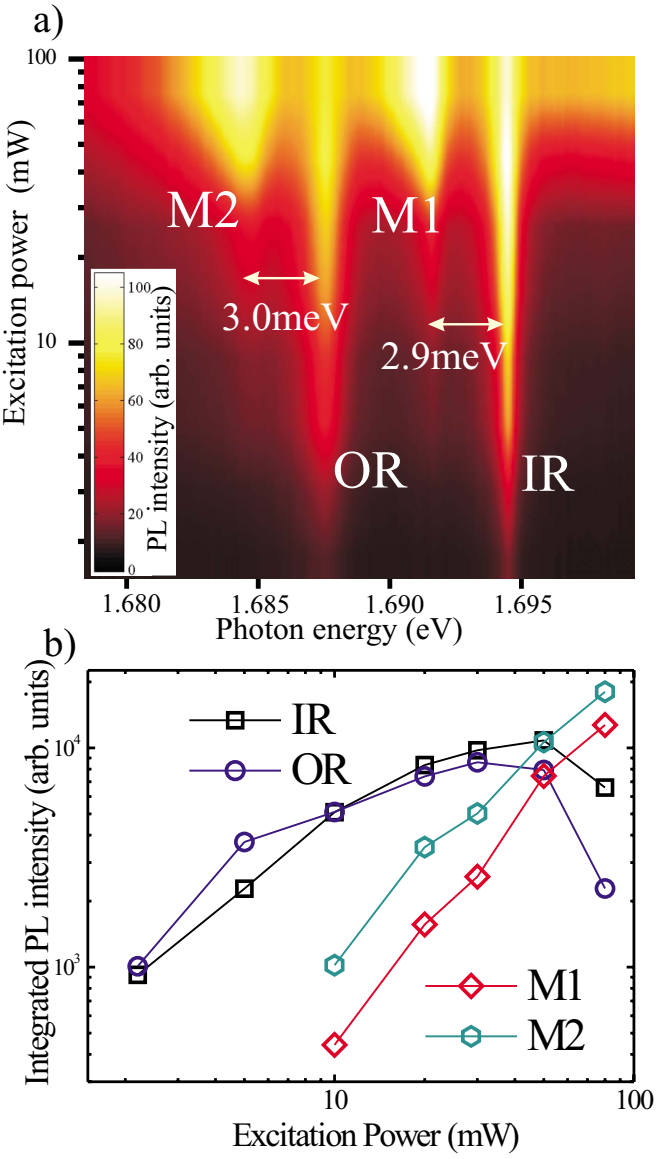

FIG. 4. (Color online) (a) Color-intensity map of a CQR power dependence. (b) Integrated PL intensity of the four contributions as a function of the excitation power.

OR not only has a larger diameter but also shows a broader width (the amplitude of the cross section) and a larger height with respect to the IR. This is fulfilled by the Gaussian fit of the CQR cross section shown in Fig. 1. The energy separation of the two lines varies depending on the considered CQR being dependent on the specific width of the IR and of the OR. Significant broadening is often measured for each line of the CQR doublet if compared with excitonic recombination in high-quality MDE GaAs quantum dots (as shown in the inset of Fig. 2). Moreover the larger value of the linewidth is usually associated to the OR contribution; IR lines as sharp as 300 μeV have been measured. Let us note that even MDE QDs may sometimes show linewidth on the order of 400 μeV.[17]

Typical second-order autocorrelation measurement for both the IR and OR emissions are shown in Figs. 3(a) and 3(b); the antibunching experiment for IR and OR was performed in the same excitation condition, avoiding saturation effects or appearance of multiexciton (MX) features in the PL spectrum (see also Fig. 4). The chosen spectral window was 0.8 meV to spectrally integrate each line. For each pulse the number of coincidence events for the two APDs is summarized in a histogram with 3 ns time bin, thus integrating over the overall time response of the system. The periodic peaks appearing at intervals of 12.2 ns indicate that photons were emitted synchronously with the pulsed excitation at 82.0 MHz. In between the PL peaks the autocorrelation value gives a precise estimate of the noise to signal ratio N/S. In particular this gives the $1-\rho^2$ value $[\rho=S/(S+N)]$ to be taken into account for a correct estimation of the $g^{(2)}(0)$.[14] This experimental value has been subtracted for the data reported in Figs. 3(a) and 3(b). We did not subtract from the histogram any other additional PL contribution.

The reduced intensity of the peak at zero time delay indicates that there is a small probability of finding more than one photon in each emitted pulse. This is the signature of a single-photon emitter under pulsed excitation. While $g^{(2)}(0)=0$ is expected for an ideal two-level system, the condition of $g^{(2)}(0)<0.5$ is required for a single-photon emitter and the

condition $g^{(2)}(0)<1$ still denotes the quantum nature of the emitter.[14,18] In our case, the correlation function at zero time delay, $g^{(2)}(0)$, is estimated to be 0.47 (± 0.15) for the IR recombination and 0.80 (± 0.13) for the OR recombination. Note that a similar experiment performed on single QD emission provides a $g^{(2)}(0)$ estimated to be 0.18 (± 0.05) without background subtraction, denoting the sensitivity of the experimental setup. The same analysis performed on several CQRs is summarized in Fig. 3(c) where the $g^{(2)}(0)$ is reported as a function of the line broadening. As expected the $g^{(2)}(0)$ increases with the increasing linewidth. Further we note that the condition $g^{(2)}(0)<0.5$ is usually fulfilled by the IR but not by the OR contribution. Finally cross correlation intensity measurements between IR and OR have been performed (not shown here). We always find $g^{(2)}_{\mathrm{IR\text{-}OR}}(0)=1$ within the experimental error. These results are not unexpected due to the independent dynamic already reported on these nanostructures.[15]

IV. DISCUSSION

The presented phenomenology poses several doubts on the possibility of using the commonly adopted picture in order to explain the PL inhomogeneous line broadening from a single nanostructure. The QD inhomogeneous line broadening is usually ascribed to quantum confined Stark effect induced by charge defects in the barrier material usually indicated as spectral diffusion (SD).[19,20] The exciton recombination energy fluctuates in a time scale much larger than the excitonic lifetime, and the line broadening is due to the pile up of different homogeneous lines during the detection time. Thus effective PL linewidth up to several hundreds of μeV can be observed in a single QD emission.[17] However this picture does imply the presence of antibunching; single QDs have been shown to be very good single-photon emitters depending less on their PL line inhomogeneous broadening. The simultaneous presence of large linewidth and $g^{(2)}(0)>0.5$ suggests that, in such case, the PL line from single CQRs is an inhomogeneous collection of different individual optical transitions. A likely explanation is that large quantum rings have to be considered as a warped analog of quantum wires. In fact, the linear extension of the outer ring of 90 nm diameter is already 280 nm long, which corresponds to a relatively long quantum wire. As a comparison let us remind that near field measurements with 150 nm resolution in quantum wires usually show a collection of sharp peaks associated to exciton center-of-mass localization.[11] The disorder may produce exciton localization in different positions along the ring.

An alternative picture for explaining the inhomogeneity of the PL lines may, in principle, consist of the presence of different excitonic complexes inside the OR PL band. In fact, while trions (T) show antibunching in cross correlation measurements, biexcitons (XX) and/or MX are in bunching with the exciton recombination.[12,13] Therefore the collection, within the 0.8 meV experimental spectral window, of XX and MX recombinations would increase the $g^{(2)}(0)$ value. In order to elucidate this point, we performed PL spectra at different excitation power reported as color-intensity map in Fig. 4. There are two relevant points. First the power dependence of both IR and OR lines is slightly sublinear which already points out that both lines are dominated by single exciton recombination. Second two new spectral components, labeled as M1 and M2, appear in the high excitation regime. The two lines present a spectral shift of 3.0 and 2.9 meV from OR and IR lines, respectively, and their power dependence is superlinear with respect to the IR and OR cases (see Fig. 4). Accordingly with time-resolved experiments[15] we attribute M1 and M2 to XX/MX recombination associated to the OR and IR, respectively. Similar behavior was reported for $GaAs/Al_{0.33}Ga_{0.67}As$ quantum wires.[21] The state filling experiment in Fig. 4 and the time-resolved analysis[15] show a saturation effect in the PL intensity and a direct transfer of charges from the excited states toward the low-lying OR and IR states. These observations exclude the presence of biexciton and exciton recombination within the IR and OR recombination lines.

We conclude that the IR is small enough to contain well-separated quantum states and gives rise to an optical transition which exhibits antibunching features. On the contrary the OR is already sufficiently large to be influenced by structural disorder, resulting in an inhomogeneously broadened emission band. Therefore, even if the disorder turns out to be an important issue for large quantum rings, we demonstrated that for sufficiently small ring diameter, MDE quantum rings can be considered as an almost ideal quantum system. This is of the utmost relevance for the exploitation, in the research of quantum computational devices, of the large variety of fascinating phenomena based on the quantum carrier confinement in circular nanostructures.

ACKNOWLEDGMENT

This work was partially supported by the Italian PRIN MIUR under Contract No. 2006022932.

*Author to whom correspondence should be addressed; abbarchi@fi.infn.it

[1] Y. Aharonov and D. Bohm, Phys. Rev. **115**, 485 (1959).

[2] N. A. J. M. Kleemans, I. M. A. Bominaar-Silkens, V. M. Fomin, V. N. Gladilin, D. Granados, A. G. Taboada, J. M. García, P. Offermans, U. Zeitler, P. C. M. Christianen, J. C. Maan, J. T. Devreese, and P. M. Koenraad, Phys. Rev. Lett. **99**, 146808 (2007).

[3] M. Grochol, F. Grosse, and R. Zimmermann, Phys. Rev. B **74**, 115416 (2006).

[4] I. R. Sellers, V. R. Whiteside, A. O. Govorov, W. C. Fan, W.-C. Chou, I. Khan, A. Petrou, and B. D. McCombe, Phys. Rev. B **77**, 241302(R) (2008).

[5] T. Mano, T. Kuroda, S. Sanguinetti, T. Ochiai, T. Tateno, J. Kim,

T. Noda, M. Kawabe, K. Sakoda, G. Kido, and N. Koguchi, Nano Lett. **5**, 425 (2005).
[6] W. H. Kuan, C. S. Tang, and C. H. Chang, Phys. Rev. B **75**, 155326 (2007).
[7] A. Lorke, R. J. Luyken, A. O. Govorov, J. P. Kotthaus, J. M. Garcia, and P. M. Petroff, Phys. Rev. Lett. **84**, 2223 (2000).
[8] A. Fuhrer, S. Lüscher, T. Ihn, T. Heinzel, K. Ensslin, W. Wegscheider, and M. Bichler, Nature (London) **413**, 822 (2001).
[9] L. G. G. V. Dias da Silva, J. M. Villas-Bôas, and S. E. Ulloa, Phys. Rev. B **76**, 155306 (2007).
[10] V. Savona, J. Phys.: Condens. Matter **19**, 295208 (2007).
[11] V. Emiliani, F. Intonti, C. Lienau, T. Elsaesser, R. Notzel, and K. H. Ploog, Phys. Rev. B **64**, 155316 (2001).
[12] T. Kuroda, M. Abbarchi, T. Mano, K. Watanabe, M. Yamagiwa, K. Kuroda, K. Sakoda, G. Kido, N. Koguchi, C. Mastrandrea, L. Cavigli, M. Gurioli, Y. Ogawa, and F. Minami, Appl. Phys. Express **1**, 042001 (2008).
[13] T. Kuroda, T. Belhadj, M. Abbarchi, C. Mastrandrea, M. Gurioli, T. Mano, N. Ikeda, Y. Sugimoto, K. Asakawa, N. Koguchi, K. Sakoda, B. Urbaszek, T. Amand, and X. Marie, Phys. Rev. B **79**, 035330 (2009).
[14] C. Becher, A. Kiraz, P. Michler, A. Imamoglu, W. V. Schoenfeld, P. M. Petroff, L. Zhang, and E. Hu, Phys. Rev. B **63**, 121312(R) (2001).
[15] S. Sanguinetti, M. Abbarchi, A. Vinattieri, M. Zamfirescu, M. Gurioli, T. Mano, T. Kuroda, and N. Koguchi, Phys. Rev. B **77**, 125404 (2008).
[16] T. Kuroda, T. Mano, T. Ochiai, S. Sanguinetti, K. Sakoda, G. Kido, and N. Koguchi, Phys. Rev. B **72**, 205301 (2005).
[17] S. Sanguinetti, E. Poliani, M. Bonfanti, M. Guzzi, E. Grilli, M. Gurioli, and N. Koguchi, Phys. Rev. B **73**, 125342 (2006).
[18] R. Loudon, *The Quantum Theory of Light*, 2nd ed. (Oxford University, New York, 1983).
[19] M. Abbarchi, F. Troiani, C. Mastrandrea, G. Goldoni, T. Kuroda, T. Mano, K. Sakoda, N. Koguchi, S. Sanguinetti, A. Vinattieri, and M. Gurioli, Appl. Phys. Lett. **93**, 162101 (2008).
[20] L. Besombes, K. Kheng, L. Marsal, and H. Mariette, Phys. Rev. B **65**, 121314(R) (2002).
[21] A. Feltrin, F. Michelini, J. L. Staehli, B. Deveaud, V. Savona, J. Toquant, X. L. Wang, and M. Ogura, Phys. Rev. Lett. **95**, 177404 (2005).